ERK5 promotes Src-induced podosome formation by limiting Rho activation

Mark Schramp,[1] Olivia Ying,[1] Tai Young Kim,[2] and G. Steven Martin[1]

[1]Department of Molecular and Cell Biology, University of California at Berkeley, Berkeley, CA 94720
[2]Department of Pharmacology, University of North Carolina at Chapel Hill, Chapel Hill, NC 27599

Increased Src activity, often associated with tumorigenesis, leads to the formation of invasive adhesions termed podosomes. Podosome formation requires the function of Rho family guanosine triphosphatases and reorganization of the actin cytoskeleton. In addition, Src induces changes in gene expression required for transformation, in part by activating mitogen-activated protein kinase (MAPK) signaling pathways. We sought to determine whether MAPK signaling regulates podosome formation. Unlike extracellular signal–regulated kinase 1/2 (ERK1/2), ERK5 is constitutively activated in Src-transformed fibroblasts. ERK5-deficient cells expressing v-Src exhibited increased RhoA activation and signaling, which lead to cellular retraction and an inability to form podosomes or induce invasion. Addition of the Rho-kinase inhibitor Y27632 to ERK5-deficient cells expressing v-Src led to cellular extension and restored podosome formation. In Src-transformed cells, ERK5 induced the expression of a Rho GTPase-activating protein (RhoGAP), RhoGAP7/DLC-1, via activation of the transcription factor myocyte enhancing factor 2C, and RhoGAP7 expression restored podosome formation in ERK5-deficient cells. We conclude that ERK5 promotes Src-induced podosome formation by inducing RhoGAP7 and thereby limiting Rho activation.

Introduction

Src is a nonreceptor tyrosine kinase that is hyperactivated in some human cancers, often in association with an increase in metastatic activity (Lutz et al., 1998; Irby and Yeatman, 2000; Rucci et al., 2006). In normal cells, Src can be activated by a variety of different stimuli, including adhesion to ECM proteins and the activation of growth factor receptors (Roche et al., 1995; Hsia et al., 2005). Many of these stimuli also result in changes in the actin cytoskeleton that require the activity of both Src and Rho GTPase family members (Ridley et al., 1992; Ridley and Hall, 1992). Like other GTPases, Rho family members cycle between an active GTP-bound state and an inactive GDP-bound state (Van Aelst and D'Souza-Schorey, 1997; Kjoller and Hall, 1999). GTP loading is facilitated by guanine nucleotide exchange factors (GEFs), and GTP hydrolysis can be catalyzed by GTPase activating proteins (GAPs; Lamarche and Hall, 1994; Cherfils and Chardin, 1999). In fibroblasts, Rho activation leads to an increase in actomyosin contractility and the formation of stress fibers (Ridley and Hall, 1992; Amano et al., 1996, 1998). The activation of Rac and CDC42, two other members of the Rho family, leads to membrane ruffling and the formation of filopodia, respectively (Ridley et al., 1992; Kozma et al., 1995).

Transformation of fibroblasts by retroviral Src (v-Src) or mutationally activated Src (SrcY527F) represents a model system for studying the mechanism by which Src activity leads to cell transformation and invasion. During tumor progression, cells gain the ability to invade other tissues, a process involving the coordination of cell migration and the secretion of extracellular proteases. Until recently, it was thought that the activation of Src led to an inhibition of Rho activity and that this decrease in Rho activity was responsible for the loss of stress fibers observed in Src-transformed cells. However, although expression of constitutively active Rho can suppress morphological transformation by Src, levels of Rho-GTP do not decrease in Src-transformed cells (Mayer et al., 1999; Pawlak and Helfman, 2002; Berdeaux et al., 2004). In addition, cycling of Rho activation is required for migration of fibroblasts, a process controlled by Src (Timpson et al., 2001). Furthermore, active Rho is required for Src-induced formation of podosomes, specialized adhesive structures that cause localized degradation of ECM proteins (Berdeaux et al., 2004).

Extracellular signal–regulated kinase 5 (ERK5), also known as Big-MAPK1 (BMK1), is a member of the MAPK family of

Correspondence to G. Steven Martin: gsm@berkeley.edu

Abbreviations used in this paper: CAT, chloramphenicol acetyl-transferase; DLC-1, deleted in liver cancer 1; ERK, extracellular signal–regulated kinase; GAP, GTPase-activating protein; GEF, guanine nucleotide exchange factor; GST, glutathione–S-transferase; MEF2, myocyte enhancing factor 2; MEK, Map and ERK kinase; MLC, myosin light chain; RBD, Rho-binding domain; ROCK, Rho kinase; ts-v-Src, temperature-sensitive v-Src.

The Rockefeller University Press $30.00
J. Cell Biol. Vol. 181 No. 7 1195–1210
www.jcb.org/cgi/doi/10.1083/jcb.200801078

serine/threonine protein kinases and can only be activated by Map and ERK kinase 5 (MEK5; Wang et al., 2005). It is unique in that it contains a C-terminal transactivation domain, allowing for a more direct role in the expression of gene targets (Kasler et al., 2000; Sohn et al., 2005). In addition, ERK5 activates many downstream proteins including members of the myocyte enhancing factor 2 (MEF2) family of transcription factors, signal transducers and activators of transcription (STATs), Myc, sap1a, serum-response element binding proteins (SREBPs), and the ribosomal protein S6 kinase (p90RSK; Kato et al., 1997; English et al., 1998; Kamakura et al., 1999; Pearson et al., 2001). Src has been shown to mediate ERK5 activation in response to a variety of different stimuli, including epidermal growth factor receptor activation, cellular exposure to asbestos, hypoxia-inducing conditions, and exposure to reactive oxygen species (Abe et al., 1997; Kato et al., 1998; Kamakura et al., 1999; Scapoli et al., 2004). ERK5 was required for focus formation in v-Src–transformed cells, and activated Src induced ERK5 nuclear translocation and MEF2-dependent gene expression (Barros and Marshall, 2005). Finally, activation of ERK5 in fibroblasts can lead to changes in the actin cytoskeleton, including a loss of stress fibers (Barros and Marshall, 2005).

We show here that ERK5 is constitutively activated in fibroblasts transformed by mutationally activated c-Src or v-Src. ERK5 was found to be required for podosome formation and for the invasive properties of cells transformed by constitutively active Src. We found that in Src-transformed cells, ERK5 induces a RhoGAP, RhoGAP7/DLC-1, thus limiting Rho activation and Rho-dependent signaling and allowing the formation of podosomes and the generation of an invasive phenotype.

Results

ERK5 is activated in Src-transformed cells

NIH3T3 cells transformed by v-Src form punctate podosomes, whereas NIH3T3 cells transformed by a mutationally activated form of c-Src (Y527F) form large podosome rosettes (Tarone et al., 1985; Lock et al., 1998). Both structures are associated with cellular invasion. ERK5 activation was increased in NIH3T3 cells expressing either SrcY527F or v-Src (Fig. 1 A). Activation of Src can lead to increased ERK1/2 activity (Maudsley et al., 2000). However, unlike the activation of ERK5, which is constitutive in Src-transformed cells (Fig. 1 A), the activation of ERK1/2 after Src activation is transient. Indeed, the levels of ERK1/2 activity were lower in the c-Src (Y527F)–transformed cells than in the untransformed parental cells (Fig. 1 A). Although the level of ERK1/2 activity is decreased, a downstream target of MAPK signaling, Fra-1, is constitutively induced in c-Src (Y527F)–transformed cells (Fig. 1 B).

To examine the effects of inhibition of MAPK signaling on Src-induced podosome formation, we initially used the c-Src (Y527F)–transformed NIH3T3 cells because of their ability to form easily visualized rosettes of podosomes. Treatment of Src-transformed cells with the MEK inhibitor U0126 inhibited both ERK1/2 and ERK5 activation and decreased Fra-1 protein levels (Fig. 1 B). Furthermore, treatment of c-Src (Y527F)–transformed NIH3T3 cells with U0126 for 24 h prevented rosette podosome formation, which indicates that MEK activity is required for Src-induced podosome formation (Fig. 1 C). Rosettes were lost after a 6-h treatment with U0126, and a loss of punctate actin structures was observed after 8 h (Fig. 1 C, top right). Rosette structures began to reappear 8 h after removal of U0126 (not depicted), and by 24 h, rosette structures and cell morphology were identical to those of untreated cells (Fig. 1 D, untreated). The delay in podosome formation after the removal of the UO126 suggested that protein synthesis is necessary for the reformation of podosomes after MEK inhibition. We tested this using cycloheximide to block de novo protein synthesis. Cells treated with cycloheximide (10 μg/ml) just before removal of U0126 did not reform podosomes but instead appeared more rounded, with strong cortical F-actin staining (Fig. 1 D, left), which indicates that reformation of podosomes in these cells required de novo protein synthesis. Similar results were obtained with another MEK inhibitor, PD 98059 (unpublished data). We conclude that activation of Src leads to ERK5 activation and that MEK activity and de novo protein synthesis are required for podosome formation in Src-transformed cells.

ERK5 is required for podosome formation in Src-transformed cells

To determine whether ERK5 was required for Src-induced podosome formation, we expressed a temperature-sensitive mutant of v-Src, ts-UP1, in ERK5 null mouse embryonic fibroblast (ERK5−/−) cells expressing an empty vector and in ERK5−/− cells reexpressing ERK5, hereinafter referred to as ERK5-FL cells (ERK5-null mouse embryonic fibroblasts stably expressing wild-type ERK5 cDNA). Pools of stable transfectants were grown for 24 h at 40°C to inhibit Src activity and then either kept at 40°C or shifted to the permissive temperature for another 24 h. Podosomes were visualized as punctate structures containing both F-actin and cortactin. Stable expression of v-Src in ERK5-FL cells caused formation of podosomes in almost 60% of the cells (Figs. 2 and 3 B). However, ERK5−/− cells stably expressing v-Src did not form podosomes and appeared rounded with strong cortical F-actin staining at the permissive temperature (Fig. 2). The punctate actin-rich structures detected in the ERK5-FL–transformed cells were also stained by an antibody against the podosome component FISH/Tks5 and by an antibody that recognizes tyrosine-phosphorylated proteins (Fig. 3 A), which confirms that these structures are podosomes. The appearance of some podosomes in ERK5-FL cells expressing ts-UP1 and grown at 40°C (Fig. 3 B) may be attributed to the leakiness of the ts-UP1 mutant, which retains residual kinase activity even at the nonpermissive temperature. We conclude that ERK5 is required for podosome formation in Src-transformed cells.

Expression of ts-UP1 led to an increase in tyrosine phosphorylation independent of ERK5 expression (Fig. 3 C). However, we observed that ERK5−/− cells expressing v-Src had higher levels of activated ERK1/2 than ERK5-FL cells expressing v-Src (Fig. 3 D). In addition, activation of temperature-sensitive v-Src (ts-v-Src) caused an increase in Fra-1 levels in both ERK5−/− and ERK5-FL cells expressing ts-v-Src (Fig. 3 D). Thus, increased ERK1/2 activation and the expression of Fra-1 are not sufficient to induce podosome formation in the absence of ERK5.

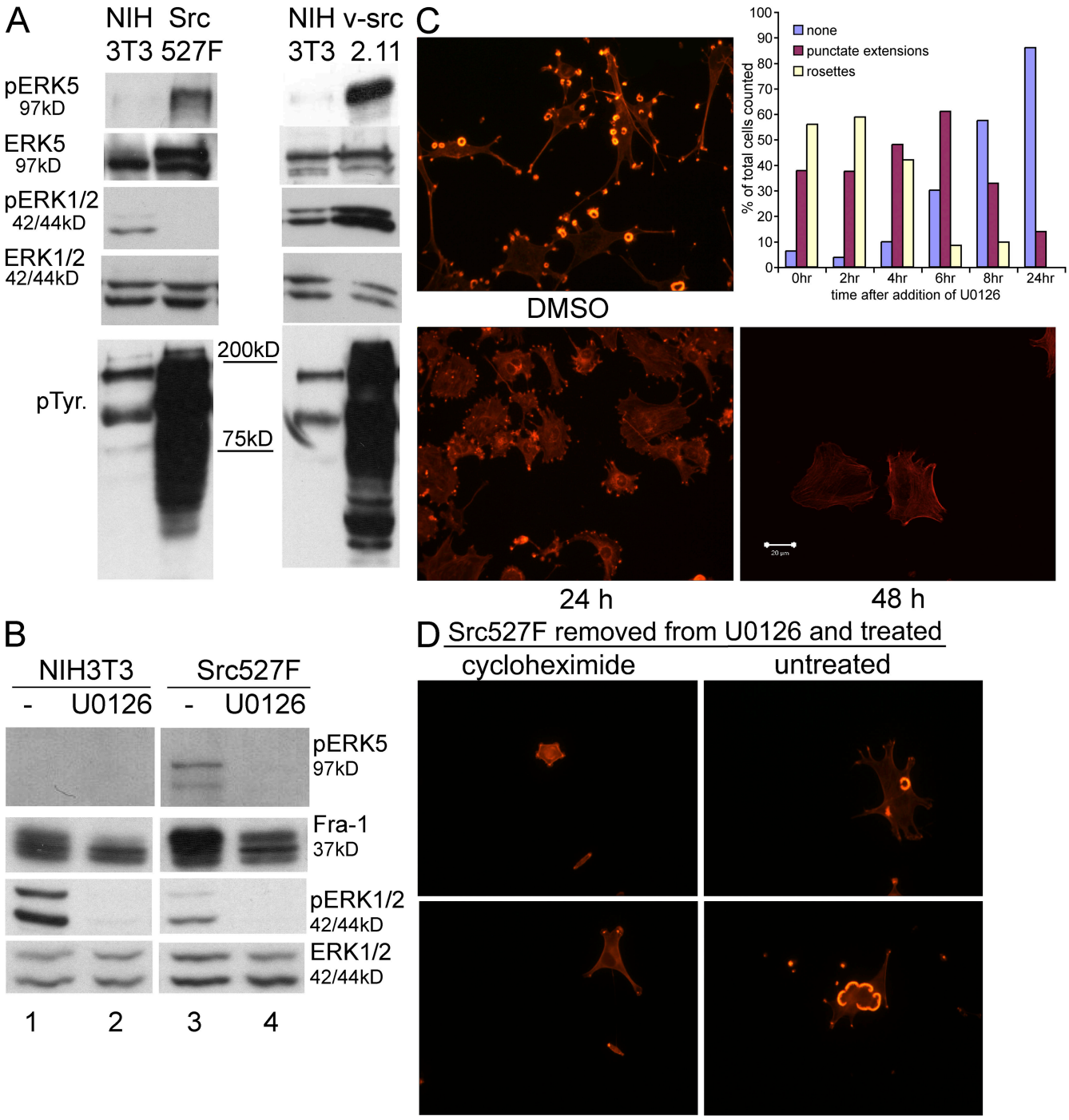

Figure 1. **MAPK signaling is required for Src induced podosome formation.** (A) NIH3T3 cells stably expressing an empty vector or SrcY527F were analyzed for ERK5, ERK1/2, and Src activity using anti–phospho-ERK5, anti–phospho-ERK1/2, or anti-phospho-tyrosine antibodies, respectively. Parental 3T3 cells expressing an empty vector or v-Src were analyzed similarly. (B) Whole cell lysates of NIH3T3 cells expressing empty vector (lanes 1–2) or c-SrcY527F (lanes 3–4) were treated with DMSO (lanes 1 and 3) or 25 μM U0126 (lanes 2 and 4) for 24 h and subjected to immunoblot analysis against the proteins indicated. (C) SrcY527F cells were treated with DMSO (top left) or 25 μM U0126 for the times indicated. Cells were fixed and stained for F-actin using rhodamine-phalloidin. Shown is a graphical representation of the percentage of cells containing rosettes, punctate actin structures, or no podosome-like structures at the indicated times after addition of U0126. All images were taken with a 40× objective lens. Bar, 20 μm. (D) Src527F cells were treated with U0126 for 24 h and then removed from the MEK inhibitor to monitor podosome reformation. 30 min before removing the inhibitor, 10 μg/ml cycloheximide was added where indicated. Cells were washed to remove the inhibitor, and fresh medium with or without cycloheximide was added as indicated. 24 h after removal of U0126, cells were fixed in 4% paraformaldehyde and stained for F-actin using rhodamine-phalloidin. Shown are two representative images. All images were taken with a 40× objective.

The invasive phenotype associated with Src transformation requires ERK5

Proteases secreted locally at podosomes degrade the ECM, allowing for cellular invasion (Linder and Aepfelbacher, 2003). We monitored protease secretion by an in situ zymography assay in which cells were plated onto an Oregon green–gelatin substrate, and protease secretion was detected by the appearance of nonfluorescent holes beneath the cell. We saw the appearance

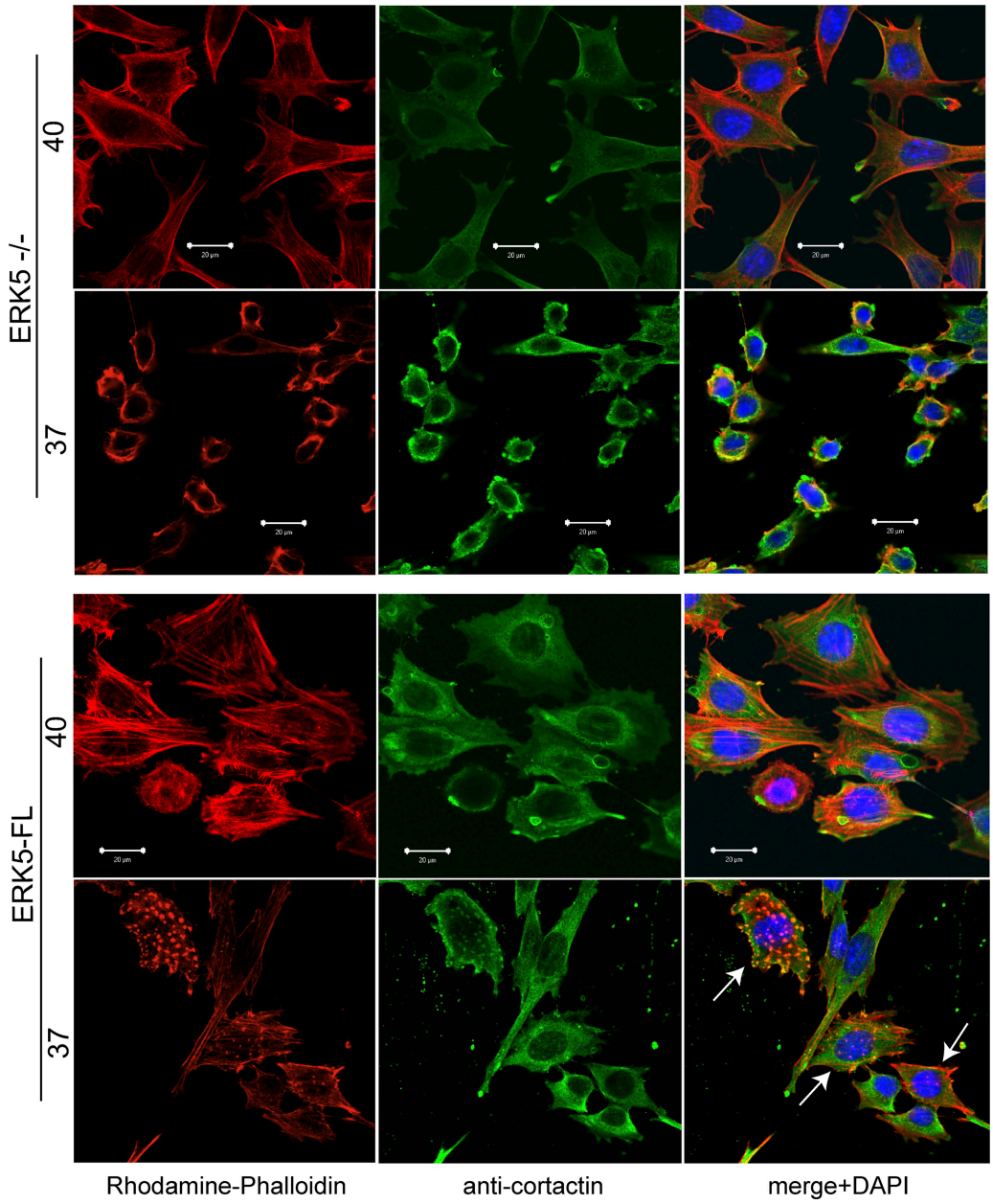

Figure 2. **ERK5−/− cells expressing ts-v-Src fail to form podosomes and become rounded with increased F-actin at the cell membrane.** ERK5−/− and ERK5-FL cells stably transfected with ts-UP1 were grown at 40°C for 24 h and then kept at 40°C (top) or shifted to 37°C (bottom) for 24 h. Cells were fixed in 4% paraformaldehyde and then stained with rhodamine-phalloidin, anti-cortactin antibody, and DAPI. Arrows indicate cells with podosomes. All images were taken with a 63× objective. Bars, 20 µm.

of nonfluorescent holes beneath >40% of the ERK5-FL ts-v-Src cells, which corresponds to the presence of punctate F-actin structures in these same cells (Fig. 4 A, bottom; and Fig. 4 B). However, <2% of ERK5−/− cells expressing ts-v-Src induced any matrix degradation (Fig. 4 A, top; and Fig. 4 B). This decrease in protease secretion resulting from ERK5 deficiency correlates with the loss of podosome formation in these cells. To investigate the effects of ERK5 deficiency on the ability of Src-transformed cells to invade in vitro, we examined the ability of ERK5−/− or ERK5-FL cells expressing ts-UP1 to migrate across transwell filters or to invade through transwell filters coated with a layer of Matrigel. The migratory properties of the two cell lines were only minimally different (Fig. 4 C, bottom). In contrast, there was a drastic reduction in the ability of ERK5−/− cells stably expressing ts-v-Src to invade through the Matrigel (Fig. 4 C, top). This suggests that the inability of ERK5−/− ts-v-Src–expressing cells to assemble podosomes blocks the invasive phenotype in Src-transformed cells.

Loss of ERK5 in v-Src-transformed cells elevates Rho-GTP loading and stimulates Rho-mediated signaling pathways

The rounded appearance and strong cortical F-actin staining in the ERK5−/− ts-UP1 cells (Fig. 2) are reminiscent of the

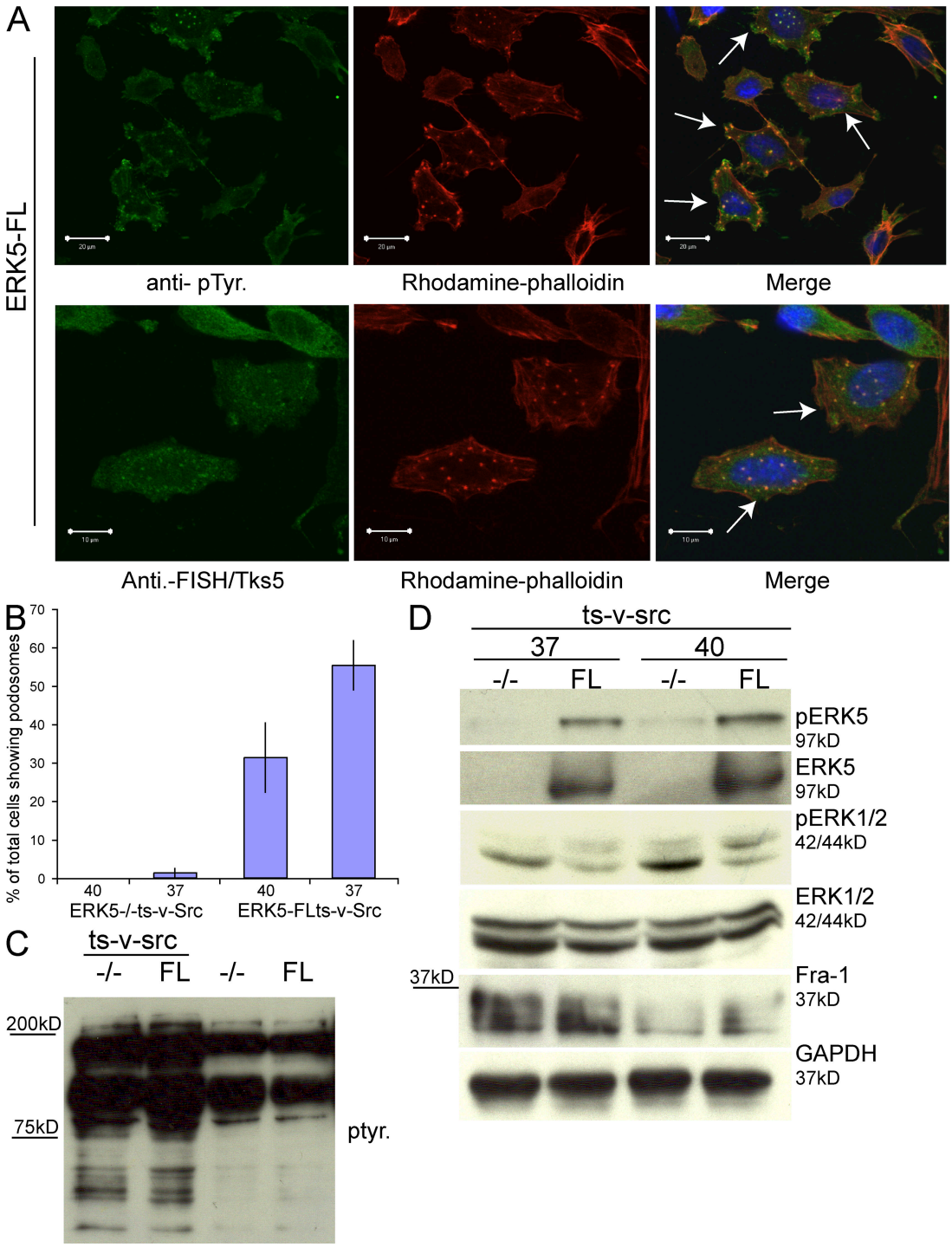

Figure 3. **ERK5−/− cells expressing ts-v-Src have increased ERK1/2 activation.** (A) Cells were treated as in Fig. 2 but stained with anti-phosphotyrosine (top) or anti-Tks5/FISH (bottom), rhodamine-phalloidin, and DAPI. All images were taken with a 63× objective. Arrows indicate cells with podosomes. Bars, 20 µm. (B) Graphical representation of the mean percentage of cells displaying podosomes over three experiments. Error bars represent SD. (C) ERK5−/− and ERK5-FL cells expressing ts-UP1 or not were monitored for Src activation by immunoblotting cellular proteins with anti-phosphotyrosine antibody. (D) ERK5-null fibroblasts and fibroblasts reexpressing ERK5 were stably transfected with a temperature-sensitive mutant of v-Src (ts-UP1). Cells were grown for 24 h at 40°C and then kept at 40° or shifted to the permissive temperature of 37° for 24 h. ERK5 and ERK1/2 were assayed by immunoblotting with anti-phosphoepitope antibodies.

phenotype that results from expression of activated Rho, and led us to hypothesize that the loss of ERK5 affects signaling by Rho. To test this, we measured the level of GTP-bound RhoA, Rac1, and CDC42 by affinity precipitation with the Rho family–specific binding domains of Rhotekin or Pak fused to glutathione–S-transferase (GST). We detected no significant difference in Rac-GTP or CDC42-GTP between v-Src–expressing cells with or without ERK5 (unpublished data). However, the level of

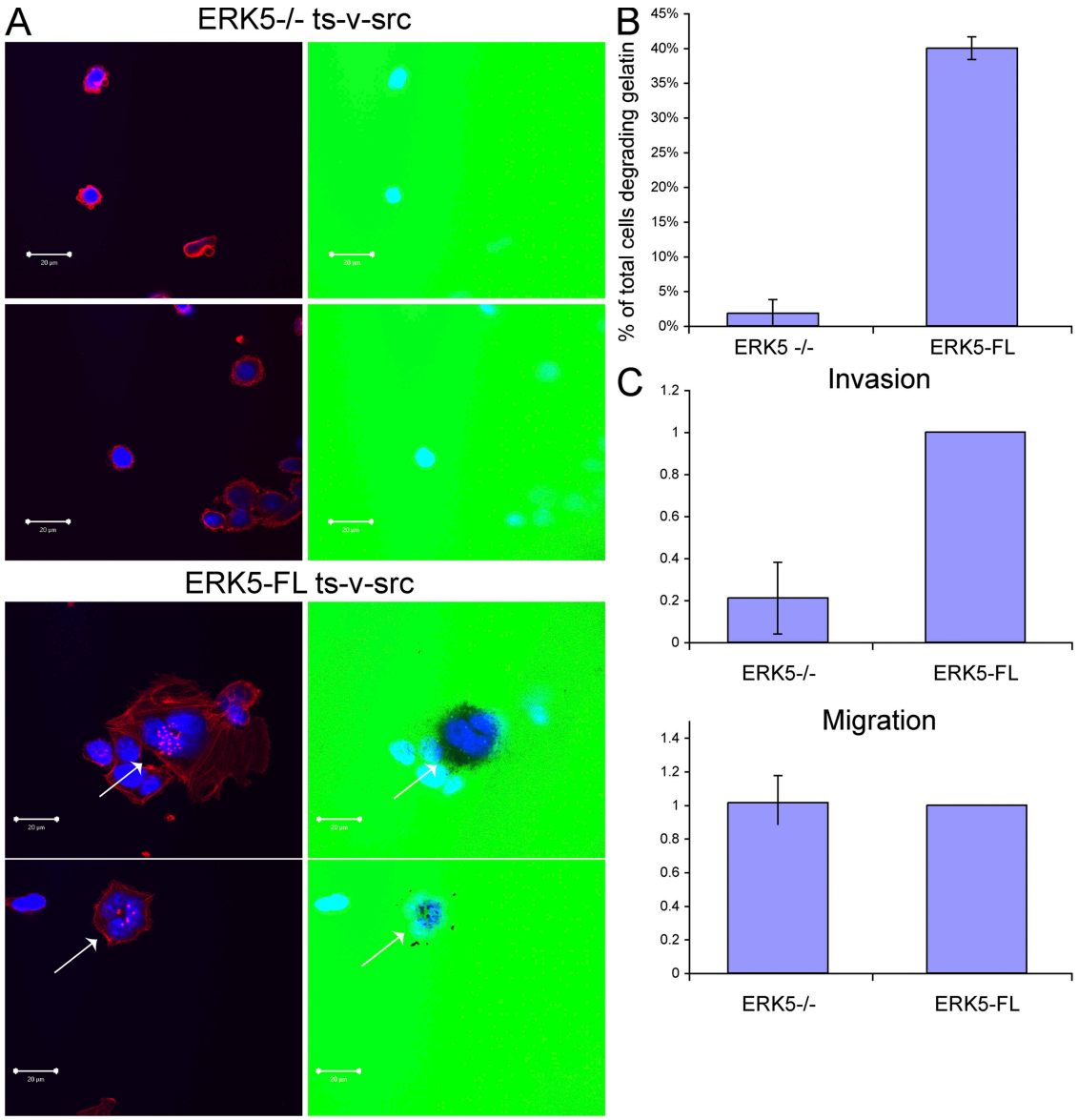

Figure 4. **Loss of ERK5 inhibits v-Src–induced ECM degradation and invasiveness.** (A) ERK5−/− and ERK5-FL cells stably transfected with ts-UP1 were plated onto coverslips coated with Oregon green–gelatin. 3 h after plating, cells were fixed and stained with rhodamine-phalloidin and DAPI (arrows indicate cells degrading Oregon green–gelatin). All images were taken with a 63× objective. Bars, 20 µm. (B) At right is a graphical representation of the mean percentage of cells counted that were degrading the gelatin matrix over four experiments. (C) ERK5−/− and ERK5-FL cells stably transfected with ts-UP1 were grown on uncoated transwell filters alone (bottom) to measure migration or on transwell filters coated with Matrigel (top) to measure invasiveness. Cells that had invaded through the filter were counted. Shown is a graphical representation of the fraction of ERK5−/− ts-UP1 cells counted relative to the number of ERK5-FL ts-UP1 cells that were counted. Error bars represent SD.

Rho-GTP in ERK5−/− ts-UP1 cells grown at 37°C was increased dramatically over the level in the ERK5-FL ts-UP1 cells (Fig. 5 A). Additionally, activation of ts-v-Src caused an increase in Rho-GTP levels in both cell lines, which is consistent with the idea that Src can lead to Rho activation. In contrast, loss of ERK5 did not significantly increase the level of Rho-GTP in cells that did not express v-Src (Fig. 5 B). We conclude that Src induces Rho-GTP loading and that the activity of ERK5 limits the extent of this activation.

GTP binding to Rho can lead to the activation of downstream effectors such as Rho kinase (ROCK). ROCK activation in turn leads to an increase in the phosphorylation of myosin light chain (MLC) either by direct phosphorylation or via activation of MLC kinase (MLCK). In parallel with the increase in Rho-GTP loading, the phosphorylation of MLC was increased in ERK5−/− ts-v-Src cells over the level observed in ERK5-FL ts-v-Src cells (Fig. 5 C, left). Thus, we conclude that the loss of ERK5 in Src-transformed cells causes a hyperelevation in the level of GTP-bound Rho, increased Rho-mediated cellular contractility, and the appearance of rounded cells.

Hyperactivation of Rho-mediated signaling pathways negatively regulates podosome formation in Src-transformed cells

We used a chemical inhibitor of ROCK (Y-27632) to determine if blocking Rho-mediated contractility could restore podosome

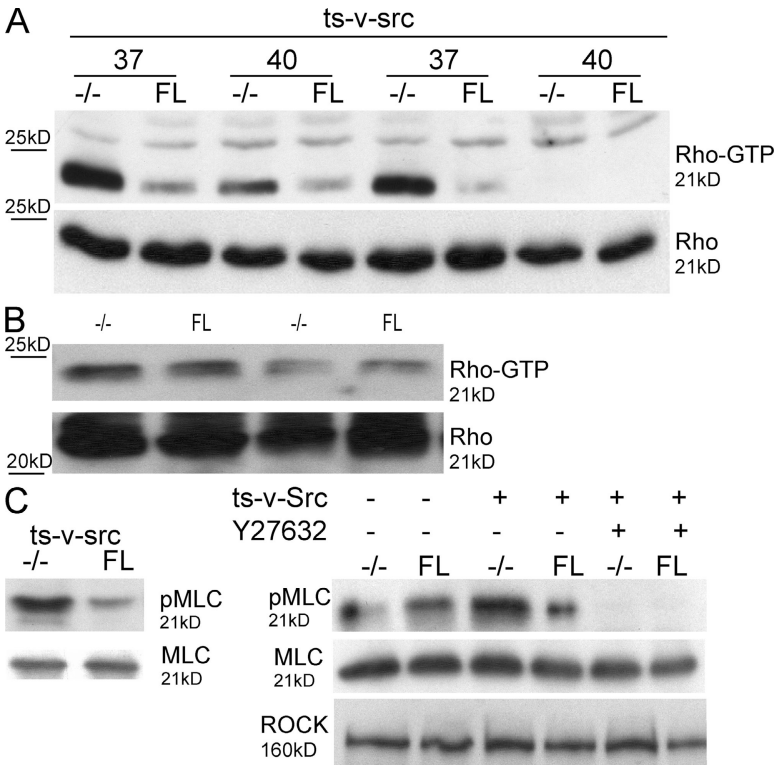

Figure 5. **Activation of RhoA and phosphorylation of MLC by v-Src are elevated in ERK5−/− cells.** (A) Affinity pull-down assays were used to determine the levels of Rho activation. ERK5−/− and ERK5-FL cells expressing ts-UP1 were grown at 40°C for 24 h and then shifted to 37°C for 24 h or kept at 40°C. Cell lysates adjusted to equal protein concentrations were incubated with GST-RBD as described in Materials and methods. The left and right portions of this blot are from separate experiments. (B) ERK5−/− and ERK5-FL cells were grown at 40°C for 24 h and then shifted to 37°C for 24 h. Rho activity was measured as described in A. (C) ERK5−/− and ERK5-FL cells stably expressing ts-UP1 were grown as in A. At the time of the shift to the permissive temperature, cells were treated with 20 μM Y-27632 where indicated. 24 h later, cells were lysed and whole cell lysates adjusted to equal protein concentrations were used to monitor MLC phosphorylation by immunoblot analysis.

formation in ERK5−/− ts-v-Src cells. Treatment of ERK5−/− or ERK5-FL cells stably expressing ts-v-Src with 20 μM Y-27632 blocked MLC phosphorylation (Fig. 5 C, right). Treatment of ERK5−/− cells expressing ts-v-Src with 20 μM Y-27632 for 24 h resulted in cell spreading (Fig. 6, middle ERK5−/− panels) and restored podosome formation in almost 35% of the cells (Fig. 6, bottom ERK5−/− panels). Treatment of ERK5-FL ts-v-Src cells with Y-27632 had little effect on cell spreading or podosome formation (Fig. 6), which is consistent with previous findings that this inhibitor does not block podosome assembly (Berdeaux et al., 2004). Treatment of ERK5−/− or ERK5-FL cells stably expressing ts-v-Src with 10 μM blebbistatin, an inhibitor of actomyosin-based contractility (Kovacs et al., 2004), for 24 h had a similar effect on cell morphology and podosome formation as treatment with Y-27632 (unpublished data). These findings suggest that hyperactivation of Rho–ROCK signaling pathways blocks cell spreading and podosome formation. To validate this conclusion, we expressed a myc-tagged constitutively active mutant of ROCK (CA-ROCK; Ishizaki et al., 1997) in Src527F-transformed 3T3 cells. Expression of CA-ROCK caused cellular rounding and a >60% reduction in the number of cells forming podosomes (Fig. 7, A and C).

To examine the effects of blocking Rho activation on cell spreading and podosome formation in ERK5-deficient cells expressing ts-UP1, we expressed a dominant-negative mutant of Rho (RhoS19N) in ERK5−/− and ERK5-FL cells expressing ts-UP1. A cotransfected GFP construct was used to identify transfected cells. Expression of DN-Rho caused the ERK5−/− cells expressing ts-v-Src to become more spread as compared with cells expressing GFP alone (Fig. 7 D, left), whereas expression of DN-Rho in ERK5-FL cells expressing ts-v-Src had little effect on cell spreading (Fig. 7 D, right). These findings provide further evidence for the conclusion that the cellular rounding phenotype observed in ERK5-deficient cells is caused by hyperactivation of Rho. In both cell lines, expression of DN-Rho suppressed podosome formation, as very few GFP-positive cells had punctate F-actin staining (Fig. 7 D), which is consistent with our previous finding (Berdeaux et al., 2004) that Rho function is required for Src-induced podosome formation. We conclude that suppression of the ROCK-dependent contractility in ERK5−/− ts-v-Src cells restores cell spreading and podosome formation. A possible explanation for the failure of DN-Rho to restore podosome formation is that some other aspect of Rho function other than ROCK-dependent actomyosin contractility is required for podosome assembly (see Discussion).

Expression of a constitutive active mutant of MEF2C limits Rho activation and restores podosome formation in ERK5−/− cells expressing ts-v-Src

The MEF2 family of transcription factors, especially MEF2C and MEF2D, has been shown to be activated by ERK5 (Kato et al., 2000). Expression of ts-UP1 caused an increase in the activity of a MEF2 transcriptional reporter in ERK5-FL cells but not in ERK5−/− cells (Fig. 8 A), which indicates that Src activates MEF2-mediated transcriptional changes and that this activation is dependent on ERK5.

To determine whether MEF2C function could rescue the defect in podosome formation resulting from ERK5 deficiency, we introduced a constitutively active mutant of MEF2C that

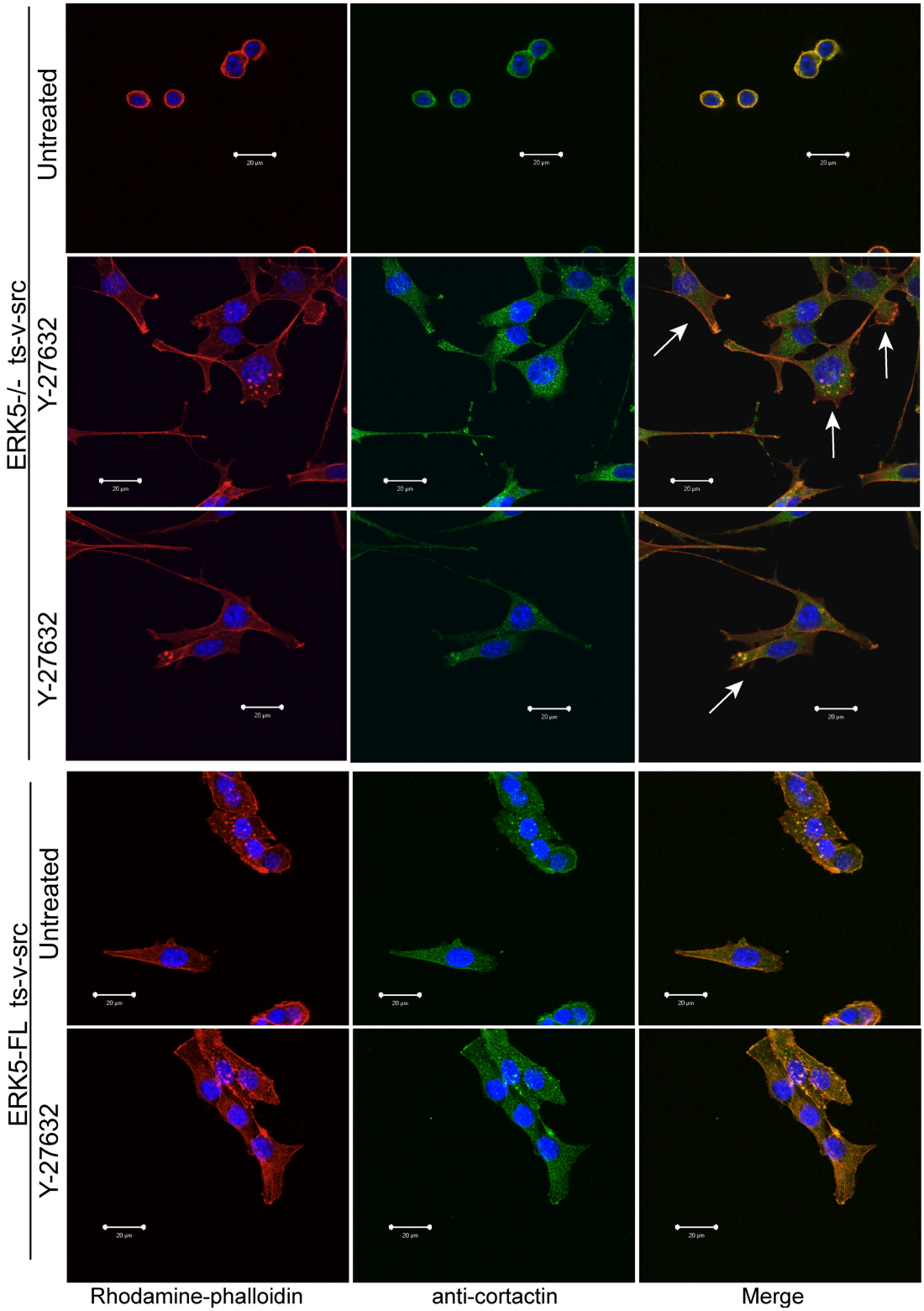

Figure 6. **Treatment of ERK5−/− v-src–expressing cells with the ROCK inhibitor Y-27632 results in cell spreading and podosome formation.** ERK5−/− and ERK5-FL cells stably transfected with ts-UP1 were treated as in Fig. 5 D. Cells were fixed and stained using rhodamine-phalloidin, anti-cortactin antibody, and DAPI (arrows indicate cells with podosomes). For the ERK5−/− ts-v-Src cells treated with the inhibitor, two images are shown. All images were taken with a 63× objective. Bars, 20 μm.

contains the DNA-binding and protein–protein interaction domains of MEF2C fused to the transactivation domain of the viral protein VP16 into ERK5−/− cells stably expressing ts-v-Src. Stable expression of the fusion protein consisting of amino acids 1–117 of MEF2C fused to the transactivation domain of VP-16 (MEF2C-VP16) resulted in an increase in cell spreading

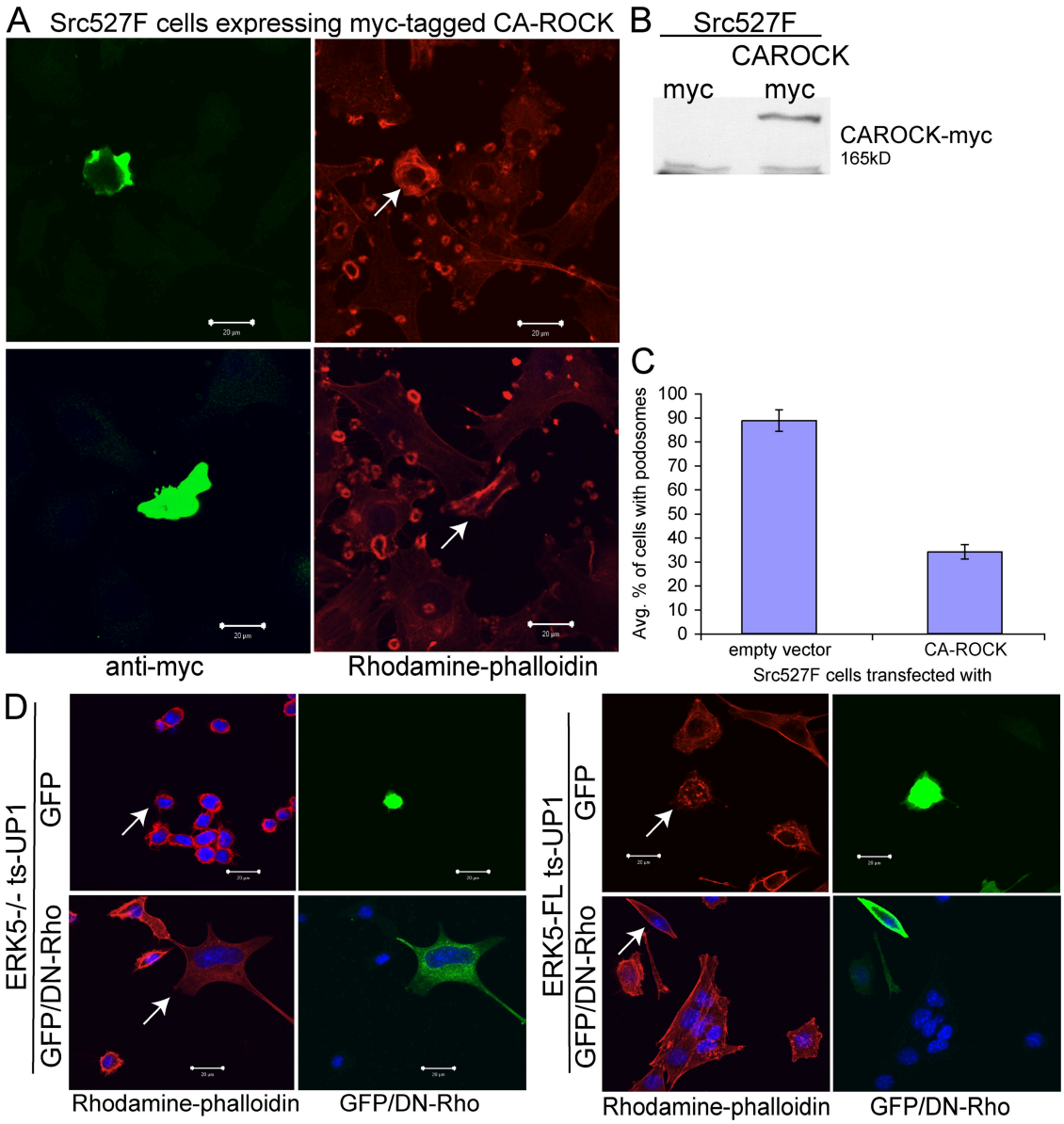

Figure 7. **Expression of a constitutively active mutant of ROCK inhibits podosome formation in Src527F-transformed cells, whereas expression of DN-RhoA in ERK5−/− ts-v-Src cells rescues cell spreading but blocks podosome formation.** (A) Src527F-transformed NIH3T3 cells were transfected with CA-ROCK-myc and plated onto glass coverslips. 24 h after plating, cells were fixed and stained with rhodamine-phalloidin and anti-myc. Arrows indicate cells expressing CA-ROCK-myc. (B) Whole cell extracts of Src527F-transformed cells transfected with an empty vector or CA-ROCK-myc were subjected to immunoblot analysis with an anti-myc antibody. (C) Shown is a graphical representation of the mean percentage of transfected cells showing podosomes (n = 3). Error bars represent SD. (D) ERK5−/− and ERK5-FL cells stably transfected with ts-UP1 were transfected with pGEX-GFP alone or with DN-RhoA and 10-fold less pGEX-GFP. Cells were plated on glass coverslips for 24 h, fixed, and stained for F-actin using rhodamine-phalloidin and DAPI. Arrows in F-actin–stained pictures indicate GFP-positive cells. All images were taken with a 63× objective. Bars, 20 μm.

in the ERK5−/− cells expressing ts-v-Src (Fig. 8 B). Furthermore, expression of MEF2C-VP16 resulted in an almost four-fold increase in the number of podosome-bearing cells (Fig. 8, B and C). Moreover, there was a dramatic decrease in the level of Rho-GTP in the cells expressing MEF2C-VP16 (Fig. 8 D). We conclude that Src activation leads to ERK5-mediated MEF2 family transcription factor activation, and that the activation of MEF2C acts to limit Rho-GTP loading, allowing the formation of podosomes. However, we cannot exclude the possibility that there may be other ERK5-dependent pathways that also act to limit Rho activation.

RhoGAP7/DLC-1 is preferentially expressed in ERK5-FL ts-v-Src cells and is required for Src-induced podosome formation

The observations described above suggested that v-Src causes ERK5-dependent gene expression and that some of the targets of this pathway act to limit Rho activation. Therefore, we performed microarray analyses on ERK5−/− and ERK5-FL cells expressing ts-v-Src to identify genes that might play a role in controlling Rho activation. These data indicated that RhoGAP7, also known as deleted in liver cancer 1 (DLC-1), was preferentially

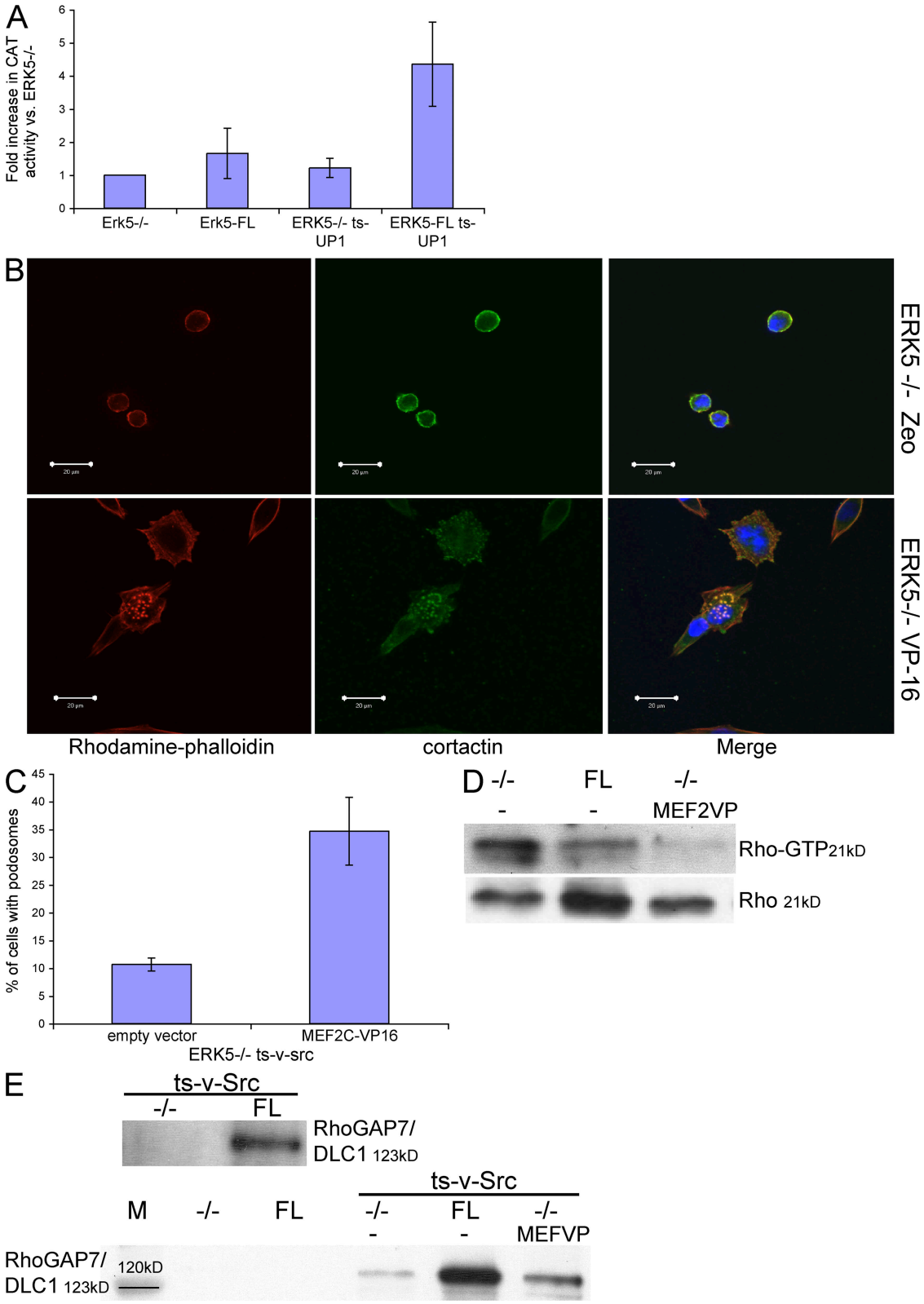

Figure 8. **Expression of MEF2C-VP16 induces podosome formation and inhibits Rho hyperactivation in ERK5−/− cells expressing v-Src.** (A) ERK5−/−, ERK5-FL, and ERK5−/− and ERK5-FL cells expressing v-Src were cotransfected with a MEF2C-CAT reporter gene and a vector expressing GFP as a transfection efficiency control. 48 h after transfection, cells were harvested and CAT activity was assayed. Numbers represent the fold increase in CAT activity normalized to GFP levels over the level observed in ERK5−/− cells. Shown is a graphical representation of the increase in CAT activity. $n = 3$ ($P < 0.05$ for ERK5-FL v-src cells compared with all other lines). (B) ERK5−/− ts-UP1 cells were stably transfected with pCDNA3.1-zeo or pCDNA3.1-zeo containing a constitutively active mutant of MEF2C, MEF2C-VP16. Cells were grown on glass coverslips for 24 h, fixed, and stained using rhodamine-phalloidin, anti-cortactin, and DAPI. All images were taken with a 63× objective. Bars, 20 µm. (C) Shown is a graphical representation of the percentage of cells that had podosomes ($n = 3$). Error bars represent SD. (D) ERK5−/− ts-UP1 cells stably transfected with an empty vector or with a vector expressing

expressed in ERK5-FL cells expressing activated ts-UP1 (unpublished data). We confirmed this result by affinity precipitation of Rho GAPs using a Rho(63L)-GST fusion protein (Garcia-Mata et al., 2006). We found that more RhoGAP7/DLC-1 was recovered from ERK5-FL cells expressing activated ts-v-Src than from ERK5−/− ts-v-Src cells (Fig. 8 E). Expression of MEF2C-VP16 also caused the level of RhoGAP7/DLC-1 to increase in ERK5−/− cells expressing activated ts-v-Src (Fig. 8 E). Additionally, in the absence of v-Src expression, neither the ERK5−/− nor the ERK5-FL cells expressed detectable levels of RhoGAP7/DLC-1 (Fig. 8 E), which indicates that its expression is a result of Src activation of ERK5. Next, we reexpressed RhoGAP7/DLC-1 in ERK5−/− ts-v-Src cells to determine if this was sufficient to restore podosome formation. We used a RhoGAP7/DLC-1–GFP fusion construct to monitor transfected cells. Expression of the RhoGAP7/DLC-1–GFP fusion protein induced the formation of podosomes in >50% of the ERK5−/− ts-v-Src cells compared with <5% in cells expressing GFP alone (Fig. 9, A and B).

To determine whether RhoGAP7/DLC-1 is required for podosome formation, we expressed a dominant-negative RhoGAP7/DLC-1–GFP fusion protein containing the N-terminal SAM domain but lacking GAP activity and the C-terminal START domain (unpublished data; Healy et al., 2008) in SrcY527F-transformed NIH3T3 cells. Expression of the DN–DLC-1–GFP inhibited podosome formation and resulted in cellular rounding (Fig. 9, C and D), which indicates that the hyperactivation of Rho that results from RhoGAP7/DLC-1 inhibition, like that resulting from ERK5-deficiency, induces a rounded cellular morphology and reduced invasive capacity. Similarly, the expression of DN–DLC-1 in ERK5-FL ts-v-Src–transformed cells reduced the number of cells that were able to form podosomes from 63% in cells expressing GFP alone to 22% (unpublished data), which confirms that RhoGAP7/DLC-1 is required for ERK5-dependent podosome formation. We conclude that Src induces RhoGAP7/DLC-1 expression via the ERK5–MEF2C pathway and that this limits Rho-GTP loading, allowing for podosome formation and cellular invasion.

Discussion

In addition to inducing autonomous cell proliferation, transformation by activated Src causes a drastic reorganization of the actin cytoskeleton. This results in the disappearance of stress fibers and the formation of podosomes, dynamic adhesions that degrade the underlying ECM and promote cellular invasion. Podosomes and the closely related structures known as invadopodia have more recently been observed in epithelial cells and carcinoma-derived tumor cell lines and appear to contribute to tumor cell invasion (Abram et al., 2003; Spinardi et al., 2004). Src is a key regulator of podosome formation in vivo, and the most prominent phenotype of Src-deficient mice is osteopetrosis, a disease caused by a defect in osteoclast podosome formation. Thus, the pathways through which Src signals to induce podosome formation and cellular invasion are of considerable interest.

The results described here indicate that the small GTPase Rho is a key regulator of Src-induced podosome formation. Because the activation of Rho is known to induce the formation of stress fibers, it was previously thought that the disappearance of these structures in Src-transformed cells was caused by a decrease in the level of Rho activation. Consistent with this hypothesis, Src has been shown to phosphorylate and possibly activate p190RhoGAP (Fincham et al., 1999). However, we and others have shown that there is no reduction in the overall level of Rho-GTP in fibroblasts transformed by SrcY527F or v-Src (Pawlak and Helfman, 2002; Berdeaux et al., 2004). Furthermore, we observe a dramatic increase in Rho-GTP levels in ERK5−/− cells expressing v-Src, which indicates that Src can activate Rho-GTP loading. The results described here lead to the model shown in Fig. 10. In this model, Src induces Rho activation, but this activation is limited by ERK5-dependent induction of RhoGAP7/DLC-1. Thus, in the absence of ERK5, Src induces hyperactivation of Rho. Rho, in turn, is necessary for podosome formation, as we and others have previously shown (Chellaiah et al., 2000; Berdeaux et al., 2004), but hyperactivation of Rho leads to elevated actomyosin contractility that blocks cell spreading and podosome formation. Thus, the relationship between Src, Rho, and podosome formation is complex. We propose a model (Fig. 10) in which Src promotes both Rho activation and Rho inactivation, and where Rho, depending on its level of activation, can either promote or inhibit podosome formation. It is possible that although the level of Rho-GTP remains unchanged in Src-transformed cells, Rho may be cycling more rapidly between the active and inactive states. Another possibility is that Src may promote Rho-GTP loading and GTP hydrolysis at different sites within the cell, leading to local Rho activation. Indeed, in Src-transformed cells, Rho activation appears to occur at podosomes (Berdeaux et al., 2004).

There are several possible mechanisms by which Src induces Rho activation. Src has been shown to directly induce Rho activation through its ability to phosphorylate Rho GDP dissociation inhibitors (RhoGDIs; DerMardirossian et al., 2006). This phosphorylation causes Rho to dissociate from RhoGDI, allowing it to translocate to the membrane. In addition, activation of RhoGEFs by Src may increase nucleotide exchange. In particular, the Rho-specific GEF Tim, a Dbl family member, is autoinhibited by an N-terminal helical motif, and phosphorylation of this motif by Src, both in vitro and in vivo, relieves this autoinhibition (Yohe et al., 2007). Src can also phosphorylate the Rho family GEFs Vav1 and Vav2 in vitro and is required for EGF-mediated activation of Vav2 (Riteau et al., 2003; Servitja et al., 2003;

MEF2C-VP16 were grown for 24 h at 40°C and then shifted to 37°C for an additional 24 h. Cells were lysed and Rho affinity pull-down assays were performed as described in the legend for Fig. 5. (E) Rho-GAP affinity binding assays were used to determine the abundance of RhoGAP7/DLC-1 in the cell lines indicated. All cell lines were grown at 40°C for 24 h and then shifted to 37°C for 24 h. Cell lysates of equal protein concentration were incubated with GST-Rho63L–bound glutathione–Sepharose beads for 1 h at 4°C. Pellets were resuspended in Laemmli buffer and RhoGAP7/DLC-1 levels were measured by immunoblot analysis (M designates the protein marker lane).

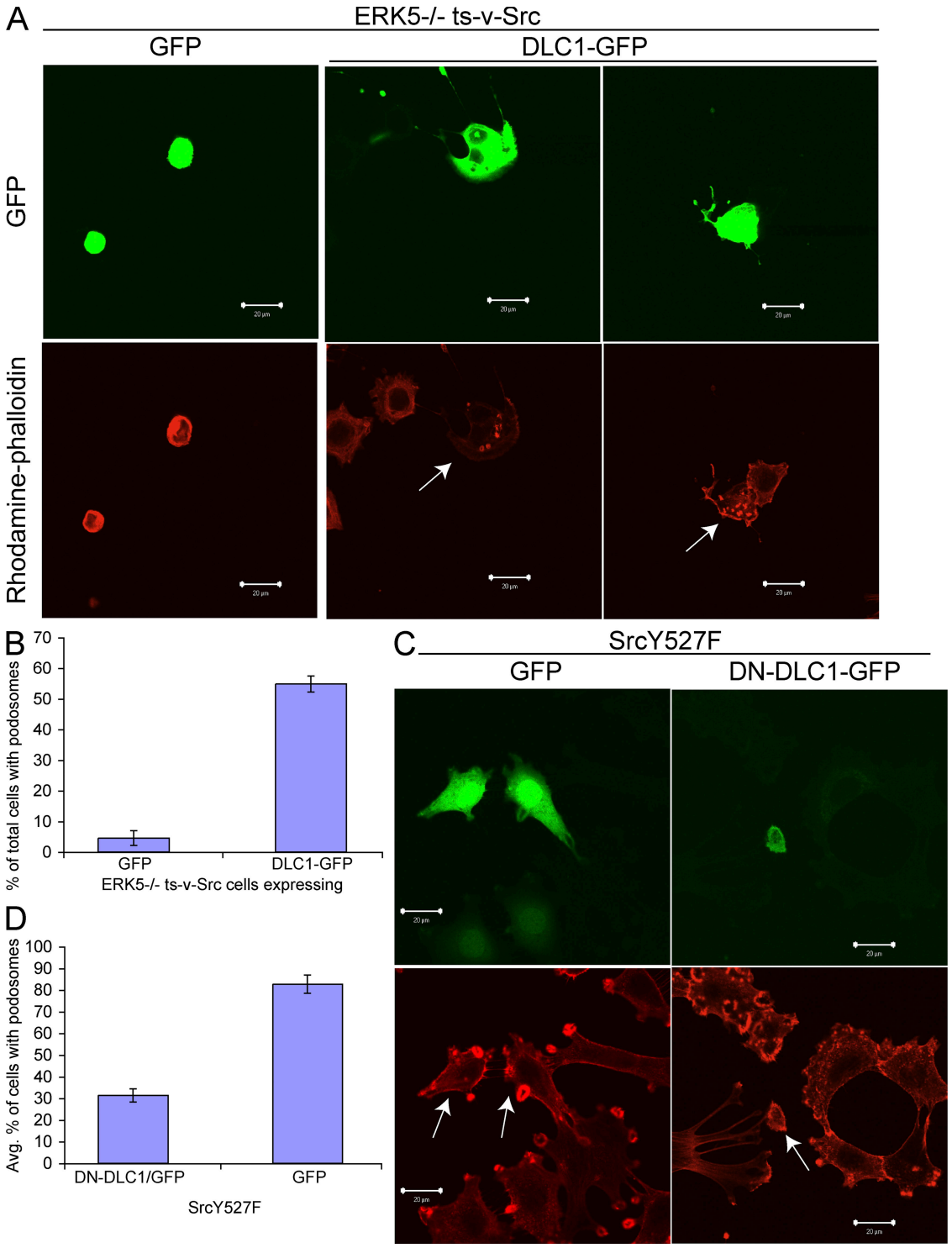

Figure 9. **RhoGAP7/DLC-1 is preferentially expressed in ERK5-FL ts-v-Src cells, and its overexpression in ERK5−/− ts-v-Src cells can restore podosome formation.** (A) ERK5−/− ts-v-Src cells were transfected with a GFP-expressing vector alone (left) or a vector encoding RhoGAP7/DLC-1–GFP fusion. Cells were plated onto glass coverslips and, 24 h later, fixed and stained with rhodamine-phalloidin. Arrows indicate cells expressing fusion protein. (B) Shown is a graphical representation of the mean percentage of cells that had podosomes (n = 3). (C) Src527F cells were transfected with DN-DLC-1–GFP or GFP alone and plated onto glass coverslips. 24 h after plating, cells were fixed and stained with rhodamine-phalloidin and DAPI. Arrows indicate cells expressing GFP or DN-DLC-1–GFP. All images were taken with a 63× objective. Bars, 20 µm. (D) Shown is a graphical representation of the mean percentage of cells that contained podosomes (n = 3). Error bars represent SD.

Stovall et al., 2004). However, Vav proteins induce GTP loading on both Rho and Rac (Han et al., 1997; Liu and Burridge, 2000; Zeng et al., 2000). Many other Rho GEFs are activated directly or indirectly by receptor tyrosine kinases (Schiller, 2006), and some of these may also be regulated by Src. Finally Src down-regulates the expression of the Cdk inhibitor p27Kip1, which

has been shown to inhibit Rho activation by blocking its interaction with Rho GEFs (Besson et al., 2004). It seems likely that phosphorylation of the RhoGDI, activation of Rho-GEFs, and down-regulation of p27Kip1 may all contribute to Src-induced Rho activation.

The phosphorylation of p190RhoGAP by Src represents one mechanism by which Src limits Rho activation. Here, we present evidence for a Src–ERK5–MEF2C pathway that also limits Rho activation by inducing the expression of RhoGAP7/DLC-1. Src can activate the classical MAP kinases ERK1 and ERK2, and their downstream target, the transcription factor Fra-1, has been shown to regulate the invasiveness of breast cancer cells as well as colon carcinoma cells through its ability to regulate Rho signaling (Vial et al., 2003; Belguise et al., 2005). However, in Src-transformed cells, ERK1/2 activation is only transient, whereas the activation of ERK5 is constitutive. ERK5 deficiency led to hyperactivation of Rho, even though both ERK1/2 activation and Fra-1 induction were observed in ERK5−/− cells expressing v-Src. Thus, ERK5 rather than ERK1/2 appears to be the critical MAPK in limiting the extent of Rho activation. This effect is mediated, at least in part, by activation of MEF2-dependent transcription. The MEF2 family of transcription factors comprises MEF2A, -B, -C, and -D, which can homo- and heterodimerize to induce gene expression (Martin et al., 1994; Black et al., 1996, 1998). MEF2-dependent signaling was enhanced in ERK5 reexpressing cells that also expressed v-Src, and the expression of MEF2C-VP16 limited Rho-GTP loading in ERK5−/− cells expressing v-Src. One major transcriptional target of the Src–ERK5–MEF2 pathway is RhoGAP7/DLC-1. RhoGAP7/DLC-1 was only induced in cells expressing v-Src; ERK5 reexpression was not sufficient to induce RhoGAP7/DLC-1 synthesis in the absence of v-Src expression. Collectively, these results indicate that one pathway that limits the extent of Rho activation in Src-transformed cells is the ERK5- and MEF2-dependent induction of RhoGAP7/DLC-1.

In the absence of ERK5, v-Src–transformed cells are rounded, with strong cortical actin staining, and lack podosomes. Cell spreading and podosome formation could be restored by reexpression of ERK5, by expression of MEF2C-VP16 or RhoGAP7/DLC-1, or by inhibition of ROCK-mediated actomyosin contractility. Thus, the hyperactivation of Rho that results from ERK5 deficiency leads to increased actomyosin contractility, and it is this that is responsible for cell rounding and podosome loss. However, blocking Rho-mediated signaling by expression of a dominant-negative RhoA mutant or with the bacterial exotoxin C3 also prevents podosome formation in Src-transformed cells (Fig. 7; Berdeaux et al., 2004). One possible explanation is that Rho signaling through some effector other than ROCK is necessary for Src-induced podosome formation. There are interesting parallels with podosome formation in osteoclasts. Mice that are deficient in Src display osteopetrosis, a disease caused by the failure of osteoclasts to resorb bone (Thomas et al., 1991). Recently, it was shown that in osteoclasts, podosome formation, structure, and dynamics are dependent on the activity of endogenous Src (Destaing et al., 2008). Osteoclast podosome formation is dependent on Rho function, and there is evidence that one of the roles of Rho in this system is to promote the formation of phosphatidylinositol-4,5-bisphosphate, thereby modulating the activity of actin-binding proteins such as gelsolin and Wiskott-Aldrich syndrome protein (WASP) (Chellaiah, 2006). It is possible that Rho may be playing a similar role in Src-transformed cells.

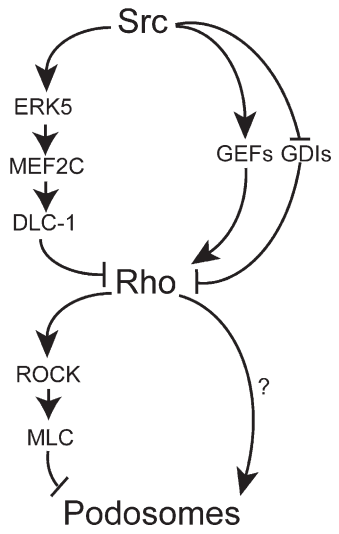

Figure 10. **Src activates pathways that lead to Rho-GTP loading and Rho-GTP hydrolysis.** Rho regulation is a key intermediate in podosome formation. Src utilizes distinct pathways to both activate and inhibit Rho. Hyperactivation of Rho can inhibit podosome formation by increasing actomyosin contractility. However, an as yet unknown aspect of Rho function is required for podosome formation.

In summary, Src induces RhoGAP7/DLC-1 expression by activating the ERK5–MEF2C pathway and thereby limiting the extent of Rho activation. The activation of this pathway is required for generation of podosomes and the invasive phenotype associated with Src transformation. Src activity is elevated in some epithelial cancers, and the extent of activation correlates with metastatic ability (Frame, 2002; Yeatman, 2004). It remains to be determined whether the Src–ERK5–MEF2C pathway plays a role in invasion by human carcinoma cells.

Materials and methods

Reagents

Anti–phospho-ERK5, anti-ERK5, and anti-MLC were obtained from Sigma-Aldrich; anti–phospho-ERK1/2 (E10) mAb, anti-ERK1/2, and anti–phospho-MLC were obtained from Cell Signaling Technology; anti-phosphotyrosine mAb (4G10) and anti-cortactin mAb (4F11) were obtained from Millipore; anti-Fra1, anti-GFP, anti-ROCK, anti-Rac1, anti-MEF2, anti-VP16, anti-CDC42, anti-myc (9E10), and anti-RhoA were obtained from Santa Cruz Biotechnology, Inc.; anti-GAPDH was obtained from Abcam; ROCK inhibitor Y27632 and blebbistatin were obtained from EMD; MEK inhibitors U0126 and PD 98,059 were obtained from Sigma-Aldrich; anti-RhoGAP7/DLC-1 was obtained from BD Biosciences; and gelatin–Oregon green 488 conjugate, anti–mouse Alexa Fluor 488 conjugate, rhodamine-phalloidin conjugates, and SlowFade reagent were obtained from Invitrogen. Anti-FISH/Tks5 was a gift from S. Courtneidge (the Burnham Institute for Medical Research, La Jolla, CA). pCAG-myc and pCAG-myc-p160ROCKΔ3 (constitutively active) were gifts from S. Narumiya (Kyoto University Faculty of Medicine, Kyoto, Japan). pEGFP-N1–DLC-1 has been described previously (Healy et al., 2008). pEGFP-N1-DN–DLC-1(1–638 amino acids) was generated using the DLC-1 cDNA (from GenBank under accession no. NM_006094) by PCR and subcloned into the BamHI site of pEGFP-N1 (BD Biosciences).

Transfection, lysate preparation, and immunoblotting

Adherent cells were transfected with Lipofectamine Plus (Invitrogen); transient transfection conditions were optimized for maximum expression and minimal toxicity. Whole-cell extracts were prepared in RIPA lysis buffer (20 mM Tris-HCl, pH 7.5, 1% sodium deoxycholate, 2 mM EDTA, 1% [vol/vol] Nonidet P-40, 150 mM NaCl, 0.1% SDS, 50 mM NaF, 0.2 mM Na_3VO_4, 10 µg/ml leupeptin, 10 µg/ml aprotinin, and 50 mM PMSF). For immunoblot analysis, proteins were resolved by SDS-PAGE and transferred to Immobilon polyvinylidene fluoride filters (Millipore). Blots were incubated 30 min in PBS-T (PBS + 0.1% Tween-20) containing 5% nonfat dry milk or 3% BSA. The blots were incubated with primary antibody overnight at 4°C, followed by incubation with HRP-conjugated secondary antibodies (Millipore), and immunolabeled proteins were visualized with Western Lightning Chemiluminescence Reagent Plus (PerkinElmer).

Cell lines

All cell lines were maintained in DME with 10% FBS. ERK5−/− and ERK5-reexpressing cells (ERK5-FL) were gifts from A. Winoto (University of California, Berkeley, Berkeley, CA). NIH3T3 parental cells and NIH3T3 cells expressing SrcY527F were gifts from S. Courtneidge. ERK5−/− and ERK5-FL cells were transfected with pBabe-hygro-ts-UP1. Resistant pools were screened for Src expression by monitoring tyrosine-phosphorylated proteins via immunoblotting. To generate cells expressing constitutively active MEF2C, ERK5−/− cells expressing ts-UP1 were stably transfected with either pCDNA3.1-zeo alone or with pCDNA3.1-zeo-MEF2C-VP16 provided by E. Olson (The University of Texas Southwestern Medical Center at Dallas, Dallas, TX). Expression of MEF2C mutants was monitored in stable transfectants by immunoblotting.

Chloramphenicol acetyl-transferase (CAT) reporter assay

pE102 MEF2-2×2 CAT reporter plasmid was obtained from E. Olson. CAT reporter assays were performed according to manufacturer's instructions for the CAT enzyme assay (Promega). Adherent cells were transfected with pE102MEF2×2CAT and 10-fold less pEGFP to monitor transfection efficiency. 48 h after transfection, cells were lysed, and aliquots containing equal amounts of protein were incubated with 25 µg n-butyryl CoA and 0.2 µCi [^{14}C]chloramphenicol (PerkinElmer). Reactions were terminated with ethyl acetate, spin-dried in a vacuum centrifuge (Speed Vac; Savant), and resuspended in equal volumes of ethyl acetate. Aliquots were spotted onto flexible TLC plates (Selecto Scientific, Inc.). Butyrylated and unbutyrylated forms of chloramphenicol were separated using chloroform/methanol (95:5) as the mobile phase and visualized by autoradiography. Amounts of butyryl-bound chloramphenicol were measured using ImageQuant software (GE Healthcare).

Immunohistochemistry

For visualization of podosomes in cells transformed by ts-v-Src, cells were plated onto glass coverslips and grown in DME supplemented with 10% FBS at 40°C for 24 h. Cells were then shifted down to the permissive temperature or maintained at 40°C for 24 h. For visualization of podosome rosettes in SrcY527F-transformed NIH3T3 cells, cells were grown on glass coverslips for 24 h and treated with DMSO or MEK inhibitor for the indicated time. Cells growing on glass coverslips were fixed in PBS plus 4% PFA for 30 min at room temperature or overnight at 4°C, permeabilized in PBS containing 0.2% Triton X-100, and incubated for 30 min in PBS containing 3% BSA and 2% normal goat serum. Samples were incubated with primary antibodies for 1 h at room temperature. Signals were developed using either Alexa Fluor 488 goat anti–rabbit or anti–mouse IgG for 1 h at room temperature. F-actin was stained using rhodamine-phalloidin for 30 min. Samples were mounted in SlowFade antifade reagent containing DAPI. Images were collected with a 40× NA 1.3 or 63× NA 1.25 objectives (Carl Zeiss, Inc.) at room temperature using a 510 confocal laser scanning microscope (LSM; Carl Zeiss, Inc.) and 510 LSM software (v. 3.2 sp2; Carl Zeiss, Inc.). DAPI was excited by a coherent enterprise laser using the 363-nm primary line; emissions from DAPI were detected using a band-pass 385–470 filter before the photomultiplier tube. Alexa Fluor 488 and Oregon green 488 were excited by an argon ion laser (LASOS) using the 488-nm primary line, and emissions were detected using a band-pass 505–550 filter before the photomultiplier tube. Rhodamine was excited by a helium neon laser using the 546-nm primary line, and emissions were detected by using a long-pass 650 filter before the photomultiplier tube. Images were exported as TIF files for subsequent processing with Photoshop version 7 (Adobe).

In situ zymography and migration/invasion assays

Oregon green–gelatin degradation assays were performed as described previously (Berdeaux et al., 2004). Results were quantified by counting cells with degrading matrix, as defined by the ability to form at least one degradation patch regardless of its size, and are represented as a percentage of the total cells counted. Migration and invasion assays were performed using BD Biocoat Control cell culture inserts (migration) or Matrigel invasion chambers (invasion; BD Biosciences). 3.8 × 10^4 cells were plated onto inserts preincubated at 37°C with DME using DME supplemented with 10% FBS as a chemoattractant. 24 h later, the cells were removed from the upper surface by scrubbing and the inserts were removed. The inserts were then fixed in 4% PFA, permeabilized with PBS containing 0.2% TritonX-100, and mounted onto coverslips using SlowFade reagent plus DAPI. Cell nuclei were counted and represented as the percentage of ERK5−/− ts-v-Src cells counted in relation to ERK5-FL ts-v-Src cells. Experiments were repeated four times.

GTPase pull-down assays

Biochemical affinity precipitation assays to measure Rho(GTP), Rac(GTP), and CDC42(GTP) were performed essentially as described previously (Ren and Schwartz, 2000). In brief, plasmids expressing GST–Rho-binding domain (RBD) or GST–p21-binding domain (PBD) were transformed into DH5α cells (Invitrogen) and expression was induced with 1 mM isopropyl β-D-1-thiogalactopyranoside for 2 h at 37°C. GST fusion proteins were purified in batch on glutathione–Sepharose 4B beads (GE Healthcare). Pull-down assays were performed with 30–60 µg of GST fusion protein and 500–800 µg of protein lysate per sample. Samples were incubated at 4°C with rocking for 1 h followed by washing five times with appropriate wash buffer for assays using GST-PBD or GST-RBD. Precipitated proteins were solubilized in SDS sample buffer and resolved by SDS-PAGE. All tubes, reagents, and rotors were prechilled on ice before use and all steps were performed in a cold room.

Rho GAP pull-down assays

Biochemical affinity pull-down assays to measure Rho GAP abundance were performed essentially as described previously (Garcia-Mata et al., 2006). Rho63L-GST plasmid constructs were obtained from K. Burridge (University of North Carolina at Chapel Hill, Chapel Hill, NC). Plasmids expressing GST-Rho63L were transformed into DH5α cells (Invitrogen) and expression was induced with 1 mM isopropyl β-D-1-thiogalactopyranoside for 3 h at 37°C. GST fusion proteins were purified in batch on glutathione–Sepharose 4B beads (GE Healthcare). Pull-down assays were performed with 30–60 µg of GST-fusion protein and 800–1,500 µg of protein lysate per sample. Samples were incubated at 4°C with rocking for 1 h followed by washing five times with lysis buffer. Precipitated proteins were then solubilized in SDS sample buffer and resolved by SDS-PAGE. All tubes, reagents, and rotors were prechilled on ice before use and all steps were performed in a cold room.

We would like to thank K. Burridge, E. Olson, S. Narumiya, S. Courtneidge, and A. Winoto for reagents and J. Donaldson, T. Prathapam, and V. Calinisan for careful reading of the manuscript.

This work was supported by National Institutes of Health grant CA17562 and the facilities of the Cancer Research Laboratory and the Biological Imaging Facility at the University of California at Berkeley. M. Schramp was supported by National Institutes of Health predoctoral fellowship 1F31CA126472.

Submitted: 14 January 2008
Accepted: 27 May 2008

References

Abe, J., M. Takahashi, M. Ishida, J.D. Lee, and B.C. Berk. 1997. c-Src is required for oxidative stress-mediated activation of big mitogen-activated protein kinase 1. *J. Biol. Chem.* 272:20389–20394.

Abram, C.L., D.F. Seals, I. Pass, D. Salinsky, L. Maurer, T.M. Roth, and S.A. Courtneidge. 2003. The adaptor protein fish associates with members of the ADAMs family and localizes to podosomes of Src-transformed cells. *J. Biol. Chem.* 278:16844–16851.

Amano, M., M. Ito, K. Kimura, Y. Fukata, K. Chihara, T. Nakano, Y. Matsuura, and K. Kaibuchi. 1996. Phosphorylation and activation of myosin by Rho-associated kinase (Rho-kinase). *J. Biol. Chem.* 271:20246–20249.

Amano, M., K. Chihara, N. Nakamura, Y. Fukata, T. Yano, M. Shibata, M. Ikebe, and K. Kaibuchi. 1998. Myosin II activation promotes neurite retraction during the action of Rho and Rho-kinase. *Genes Cells.* 3:177–188.

Barros, J.C., and C.J. Marshall. 2005. Activation of either ERK1/2 or ERK5 MAP kinase pathways can lead to disruption of the actin cytoskeleton. *J. Cell Sci.* 118:1663–1671.

Belguise, K., N. Kersual, F. Galtier, and D. Chalbos. 2005. FRA-1 expression level regulates proliferation and invasiveness of breast cancer cells. *Oncogene.* 24:1434–1444.

Berdeaux, R.L., B. Diaz, L. Kim, and G.S. Martin. 2004. Active Rho is localized to podosomes induced by oncogenic Src and is required for their assembly and function. *J. Cell Biol.* 166:317–323.

Besson, A., M. Gurian-West, A. Schmidt, A. Hall, and J.M. Roberts. 2004. p27Kip1 modulates cell migration through the regulation of RhoA activation. *Genes Dev.* 18:862–876.

Black, B.L., K.L. Ligon, Y. Zhang, and E.N. Olson. 1996. Cooperative transcriptional activation by the neurogenic basic helix-loop-helix protein MASH1 and members of the myocyte enhancer factor-2 (MEF2) family. *J. Biol. Chem.* 271:26659–26663.

Black, B.L., J.D. Molkentin, and E.N. Olson. 1998. Multiple roles for the MyoD basic region in transmission of transcriptional activation signals and interaction with MEF2. *Mol. Cell. Biol.* 18:69–77.

Chellaiah, M., N. Kizer, M. Silva, U. Alvarez, D. Kwiatkowski, and K.A. Hruska. 2000. Gelsolin deficiency blocks podosome assembly and produces increased bone mass and strength. *J. Cell Biol.* 148:665–678.

Chellaiah, M.A. 2006. Regulation of podosomes by integrin alphavbeta3 and Rho GTPase-facilitated phosphoinositide signaling. *Eur. J. Cell Biol.* 85:311–317.

Cherfils, J., and P. Chardin. 1999. GEFs: structural basis for their activation of small GTP-binding proteins. *Trends Biochem. Sci.* 24:306–311.

DerMardirossian, C., G. Rocklin, J.Y. Seo, and G.M. Bokoch. 2006. Phosphorylation of RhoGDI by Src regulates Rho GTPase binding and cytosol-membrane cycling. *Mol. Biol. Cell.* 17:4760–4768.

Destaing, O., A. Sanjay, C. Itzstein, W.C. Horne, D. Toomre, P.D. Camilli, and R. Baron. 2008. The tyrosine kinase activity of c-Src regulates actin dynamics and organization of podosomes in osteoclasts. *Mol. Biol. Cell.* 19:394–404.

English, J.M., G. Pearson, R. Baer, and M.H. Cobb. 1998. Identification of substrates and regulators of the mitogen-activated protein kinase ERK5 using chimeric protein kinases. *J. Biol. Chem.* 273:3854–3860.

Fincham, V.J., A. Chudleigh, and M.C. Frame. 1999. Regulation of p190 Rho-GAP by v-Src is linked to cytoskeletal disruption during transformation. *J. Cell Sci.* 112(Pt 6):947–956.

Frame, M.C. 2002. Src in cancer: deregulation and consequences for cell behaviour. *Biochim. Biophys. Acta.* 1602:114–130.

Garcia-Mata, R., K. Wennerberg, W.T. Arthur, N.K. Noren, S.M. Ellerbroek, and K. Burridge. 2006. Analysis of activated GAPs and GEFs in cell lysates. *Methods Enzymol.* 406:425–437.

Han, J., B. Das, W. Wei, L. Van Aelst, R.D. Mosteller, R. Khosravi-Far, J.K. Westwick, C.J. Der, and D. Broek. 1997. Lck regulates Vav activation of members of the Rho family of GTPases. *Mol. Cell. Biol.* 17:1346–1353.

Healy, K.D., L. Hodgson, T.Y. Kim, A. Shutes, S. Maddileti, R.L. Juliano, K.M. Hahn, T.K. Harden, Y.J. Bang, and C.J. Der. 2008. DLC-1 suppresses non-small cell lung cancer growth and invasion by RhoGAP-dependent and independent mechanisms. *Mol. Carcinog.* 47:326–337.

Hsia, D.A., S.T. Lim, J.A. Bernard-Trifilo, S.K. Mitra, S. Tanaka, J. den Hertog, D.N. Streblow, D. Ilic, M.H. Ginsberg, and D.D. Schlaepfer. 2005. Integrin alpha4beta1 promotes focal adhesion kinase-independent cell motility via alpha4 cytoplasmic domain-specific activation of c-Src. *Mol. Cell. Biol.* 25:9700–9712.

Irby, R.B., and T.J. Yeatman. 2000. Role of Src expression and activation in human cancer. *Oncogene.* 19:5636–5642.

Ishizaki, T., M. Naito, K. Fujisawa, M. Maekawa, N. Watanabe, Y. Saito, and S. Narumiya. 1997. p160ROCK, a Rho-associated coiled-coil forming protein kinase, works downstream of Rho and induces focal adhesions. *FEBS Lett.* 404:118–124.

Kamakura, S., T. Moriguchi, and E. Nishida. 1999. Activation of the protein kinase ERK5/BMK1 by receptor tyrosine kinases. Identification and characterization of a signaling pathway to the nucleus. *J. Biol. Chem.* 274:26563–26571.

Kasler, H.G., J. Victoria, O. Duramad, and A. Winoto. 2000. ERK5 is a novel type of mitogen-activated protein kinase containing a transcriptional activation domain. *Mol. Cell. Biol.* 20:8382–8389.

Kato, Y., V.V. Kravchenko, R.I. Tapping, J. Han, R.J. Ulevitch, and J.D. Lee. 1997. BMK1/ERK5 regulates serum-induced early gene expression through transcription factor MEF2C. *EMBO J.* 16:7054–7066.

Kato, Y., R.I. Tapping, S. Huang, M.H. Watson, R.J. Ulevitch, and J.D. Lee. 1998. Bmk1/Erk5 is required for cell proliferation induced by epidermal growth factor. *Nature.* 395:713–716.

Kato, Y., M. Zhao, A. Morikawa, T. Sugiyama, D. Chakravortty, N. Koide, T. Yoshida, R.I. Tapping, Y. Yang, T. Yokochi, and J.D. Lee. 2000. Big mitogen-activated kinase regulates multiple members of the MEF2 protein family. *J. Biol. Chem.* 275:18534–18540.

Kjoller, L., and A. Hall. 1999. Signaling to Rho GTPases. *Exp. Cell Res.* 253:166–179.

Kovacs, M., J. Toth, C. Hetenyi, A. Malnasi-Csizmadia, and J.R. Sellers. 2004. Mechanism of blebbistatin inhibition of myosin II. *J. Biol. Chem.* 279:35557–35563.

Kozma, R., S. Ahmed, A. Best, and L. Lim. 1995. The Ras-related protein Cdc42Hs and bradykinin promote formation of peripheral actin microspikes and filopodia in Swiss 3T3 fibroblasts. *Mol. Cell. Biol.* 15:1942–1952.

Lamarche, N., and A. Hall. 1994. GAPs for rho-related GTPases. *Trends Genet.* 10:436–440.

Linder, S., and M. Aepfelbacher. 2003. Podosomes: adhesion hot-spots of invasive cells. *Trends Cell Biol.* 13:376–385.

Liu, B.P., and K. Burridge. 2000. Vav2 activates Rac1, Cdc42, and RhoA downstream from growth factor receptors but not beta1 integrins. *Mol. Cell. Biol.* 20:7160–7169.

Lock, P., C.L. Abram, T. Gibson, and S.A. Courtneidge. 1998. A new method for isolating tyrosine kinase substrates used to identify fish, an SH3 and PX domain-containing protein, and Src substrate. *EMBO J.* 17:4346–4357.

Lutz, M.P., I.B. Esser, B.B. Flossmann-Kast, R. Vogelmann, H. Luhrs, H. Friess, M.W. Buchler, and G. Adler. 1998. Overexpression and activation of the tyrosine kinase Src in human pancreatic carcinoma. *Biochem. Biophys. Res. Commun.* 243:503–508.

Martin, J.F., J.M. Miano, C.M. Hustad, N.G. Copeland, N.A. Jenkins, and E.N. Olson. 1994. A Mef2 gene that generates a muscle-specific isoform via alternative mRNA splicing. *Mol. Cell. Biol.* 14:1647–1656.

Maudsley, S., K.L. Pierce, A.M. Zamah, W.E. Miller, S. Ahn, Y. Daaka, R.J. Lefkowitz, and L.M. Luttrell. 2000. The beta(2)-adrenergic receptor mediates extracellular signal-regulated kinase activation via assembly of a multi-receptor complex with the epidermal growth factor receptor. *J. Biol. Chem.* 275:9572–9580.

Mayer, T., M. Meyer, A. Janning, A.C. Schiedel, and A. Barnekow. 1999. A mutant form of the rho protein can restore stress fibers and adhesion plaques in v-src transformed fibroblasts. *Oncogene.* 18:2117–2128.

Pawlak, G., and D.M. Helfman. 2002. MEK mediates v-Src-induced disruption of the actin cytoskeleton via inactivation of the Rho-ROCK-LIM kinase pathway. *J. Biol. Chem.* 277:26927–26933.

Pearson, G., J.M. English, M.A. White, and M.H. Cobb. 2001. ERK5 and ERK2 cooperate to regulate NF-kappaB and cell transformation. *J. Biol. Chem.* 276:7927–7931.

Ren, X.D., and M.A. Schwartz. 2000. Determination of GTP loading on Rho. *Methods Enzymol.* 325:264–272.

Ridley, A.J., and A. Hall. 1992. The small GTP-binding protein rho regulates the assembly of focal adhesions and actin stress fibers in response to growth factors. *Cell.* 70:389–399.

Ridley, A.J., H.F. Paterson, C.L. Johnston, D. Diekmann, and A. Hall. 1992. The small GTP-binding protein rac regulates growth factor-induced membrane ruffling. *Cell.* 70:401–410.

Riteau, B., D.F. Barber, and E.O. Long. 2003. Vav1 phosphorylation is induced by beta2 integrin engagement on natural killer cells upstream of actin cytoskeleton and lipid raft reorganization. *J. Exp. Med.* 198:469–474.

Roche, S., M. Koegl, M.V. Barone, M.F. Roussel, and S.A. Courtneidge. 1995. DNA synthesis induced by some but not all growth factors requires Src family protein tyrosine kinases. *Mol. Cell. Biol.* 15:1102–1109.

Rucci, N., I. Recchia, A. Angelucci, M. Alamanou, A. Del Fattore, D. Fortunati, M. Susa, D. Fabbro, M. Bologna, and A. Teti. 2006. Inhibition of protein kinase c-Src reduces the incidence of breast cancer metastases and increases survival in mice: implications for therapy. *J. Pharmacol. Exp. Ther.* 318:161–172.

Scapoli, L., M.E. Ramos-Nino, M. Martinelli, and B.T. Mossman. 2004. Src-dependent ERK5 and Src/EGFR-dependent ERK1/2 activation is required for cell proliferation by asbestos. *Oncogene.* 23:805–813.

Schiller, M.R. 2006. Coupling receptor tyrosine kinases to Rho GTPases–GEFs what's the link. *Cell. Signal.* 18:1834–1843.

Servitja, J.M., M.J. Marinissen, A. Sodhi, X.R. Bustelo, and J.S. Gutkind. 2003. Rac1 function is required for Src-induced transformation. Evidence of a role for Tiam1 and Vav2 in Rac activation by Src. *J. Biol. Chem.* 278:34339–34346.

Sohn, S.J., D. Li, L.K. Lee, and A. Winoto. 2005. Transcriptional regulation of tissue-specific genes by the ERK5 mitogen-activated protein kinase. *Mol. Cell. Biol.* 25:8553–8566.

Spinardi, L., J. Rietdorf, L. Nitsch, M. Bono, C. Tacchetti, M. Way, and P.C. Marchisio. 2004. A dynamic podosome-like structure of epithelial cells. *Exp. Cell Res.* 295:360–374.

Stovall, S.H., A.K. Yi, E.A. Meals, A.J. Talati, S.A. Godambe, and B.K. English. 2004. Role of vav1- and src-related tyrosine kinases in macrophage activation by CpG DNA. *J. Biol. Chem.* 279:13809–13816.

Tarone, G., D. Cirillo, F.G. Giancotti, P.M. Comoglio, and P.C. Marchisio. 1985. Rous sarcoma virus-transformed fibroblasts adhere primarily at discrete protrusions of the ventral membrane called podosomes. *Exp. Cell Res.* 159:141–157.

Thomas, J.E., P. Soriano, and J.S. Brugge. 1991. Phosphorylation of c-Src on tyrosine 527 by another protein tyrosine kinase. *Science.* 254:568–571.

Timpson, P., G.E. Jones, M.C. Frame, and V.G. Brunton. 2001. Coordination of cell polarization and migration by the Rho family GTPases requires Src tyrosine kinase activity. *Curr. Biol.* 11:1836–1846.

Van Aelst, L., and C. D'Souza-Schorey. 1997. Rho GTPases and signaling networks. *Genes Dev.* 11:2295–2322.

Vial, E., E. Sahai, and C.J. Marshall. 2003. ERK-MAPK signaling coordinately regulates activity of Rac1 and RhoA for tumor cell motility. *Cancer Cell.* 4:67–79.

Wang, X., A.J. Merritt, J. Seyfried, C. Guo, E.S. Papadakis, K.G. Finegan, M. Kayahara, J. Dixon, R.P. Boot-Handford, E.J. Cartwright, et al. 2005. Targeted deletion of mek5 causes early embryonic death and defects in the extracellular signal-regulated kinase 5/myocyte enhancer factor 2 cell survival pathway. *Mol. Cell. Biol.* 25:336–345.

Yeatman, T.J. 2004. A renaissance for SRC. *Nat. Rev. Cancer.* 4:470–480.

Yohe, M.E., K.L. Rossman, O.S. Gardner, A.E. Karnoub, J.T. Snyder, S. Gershburg, L.M. Graves, C.J. Der, and J. Sondek. 2007. Auto-inhibition of the Dbl family protein Tim by an N-terminal helical motif. *J. Biol. Chem.* 282:13813–13823.

Zeng, L., P. Sachdev, L. Yan, J.L. Chan, T. Trenkle, M. McClelland, J. Welsh, and L.H. Wang. 2000. Vav3 mediates receptor protein tyrosine kinase signaling, regulates GTPase activity, modulates cell morphology, and induces cell transformation. *Mol. Cell. Biol.* 20:9212–9224.